Contemporary Mathematics
http://ojs.wiserpub.com/index.php/CM/

Research Article

Topological Analysis of Fractal Binary and Ternary Trees

Thanga Rajeswari K, Manimaran A*

Department of Mathematics, School of Advanced Sciences, Vellore Institute of Technology, Vellore, 632014, Tamil Nadu, India
E-mail: manimaran.a@vit.ac.in

Received: 21 October 2024; **Revised:** 2 January 2025; **Accepted:** 2 January 2025

Abstract: Fractals are complex geometric objects that seem the same at different scales and have self-similarity. Because of this special characteristic, fractals can be used to simulate intricate biological processes. Fractal binary and ternary trees are novel data types that combine the productiveness of tree architectures with the ideas of fractal geometry. In addition to self-similarity and scalability, these trees have potential across a range of computer science and medical applications. The main goal of the study is to identify and analyze topological indices and graph entropy for fractal binary and fractal ternary trees. By examining indices such as the Randić index, Zagreb indices, and entropy measurements, the study aims to obtain a comprehensive knowledge of the structural complexity and information-theoretic properties of these fractal graphs. The study starts with the vertex and edge partitioning of fractal binary and ternary trees in order to distinguish different structural classes. Using these partitions, we obtained topological indices and graph entropy values for the fractal trees. Also, this study compares the topological indices for each fractal tree with the number of copies in the fractal dimension for a succession of graphs.

***Keywords*:** topological descriptors, entropy, fractal binary tree, fractal ternary tree

MSC: 05C92, 92E10, 28A80

1. Introduction

Mandelbrot [1] initially proposed and gave the name for the recently emerging field of fractals, which is used to investigate nature and atypical images and patterns. Fractal geometry is a branch of mathematics that studies shapes and patterns that exhibit self-similarity across different scales. Because they provide a glimpse into the limitless complexity of geometric patterns, fractals have captivated scholars for millennia. While fractal geometry deals with complicated, irregular structures that are hard to explain with conventional algebraic notions, traditional Euclidean geometry concentrates on standard structures like triangles, squares, and circles. Usually, fractals are produced by iterative procedures in which a fundamental principle is used over and over to produce a design that gets more intricate. Fractals are scale-invariant, meaning that no matter how much they are magnified, their structure stays the same. The understanding and modeling of intricate structures in mathematics and nature have been completely transformed by fractal geometry. Its ideas are not simply intriguing, but they also have broad applications in many different fields of science and engineering. Fractals provide a special lens by which it is possible to see the endless diversity of life around us whenever we strive to investigate the geometric reality.

Copyright ©2025 Manimaran A, et al.
DOI: https://doi.org/10.37256/cm.6120255952
This is an open-access article distributed under a CC BY license
(Creative Commons Attribution 4.0 International License)
https://creativecommons.org/licenses/by/4.0/

The idea of fractal dimension was first presented by mathematician Benoit Mandelbrot in his book "The Fractal Geometry of Nature" [1]. In order to describe the intricacy of fractal structures, Mandelbrot proposed the fractal dimension, which allows observations to demonstrate how a fractal intricacy changes with scale. A fundamental framework for deciphering the physical characteristics of erratic and self-similar structures in fractal geometry is provided by this concept. The ability of a fractal to appear identical at various scales is known as self-similarity. This indicates that every tiny portion of the fractal is either precisely or nearly like the whole. We can use this vital variable to characterize a wide range of objects, including data sets and time series. Scalability in fractal geometry refers to the ability of a fractal to maintain its structural complexity or pattern under different magnifications. The amount that determines whether the fractal dimension shrinks or grows over each repetition is known as the scaling factor. Together, self-similarity and scalability define the recursive and infinite complexity of fractals, making them distinct from traditional geometric objects. Since fractal objects have non-integer fractional dimensions, they seem the same under various magnification levels. With N representing the number of self-similar components at every repetition and S representing the scaling factor, the similarity dimension formula for self-similar fractals will be employed to generate the fractal dimension FD.

$$FD = \frac{log(N)}{log(S)} \tag{1}$$

A unique kind of fractal that graphically depicts the design of a binary tree, in which every node splits into two tiny nodes, is a fractal binary tree [2, 3]. Unlike the usual binary trees utilized in computer science, which are abstract data structures, a fractal binary tree is a geometrical form that is produced by a sequential method. The angle where every branch emerges from the trunk is a significant factor called the branching angle. The fractal binary tree looks consistent if the branching angle is throughout unique, and the tree looks inconsistent if the branching angle is distinct. The scaling factor defines the width of the branches. The scaling factor employed affects the thickness and complexity of the tree.

A fractal binary tree generates a large variety of fractals by merely altering the scaling factor and branching angle. The fractal binary tree imitates a wide range of designs in nature by configuring its parameters. Figure 1 depicts a symmetric binary tree with a branching angle of 45° and a scaling factor of $\frac{1}{\sqrt{2}}$. The branch extremities form a fractal that matches the Lévy Dragon. Figure 2 demonstrates a golden 144° symmetric binary tree with a branching angle of 144° and a scaling factor of $\frac{2}{1+\sqrt{5}}$. Four further copies of the tree are rotated by 72° around the bottom of the trunk, and their branch ends will create a Golden Koch snowflake. They are the Golden Koch Snowflake, Lévy Dragon, Peano Curve, Barnsley Fern, H-Tree fractal, Sierpiński Triangle, Vicsek fractal, Apollonian Gasket, Hilbert Curve, and so on. Considering modifications to the branching angle, recursion rules, and scaling factor, the fractal binary tree can produce a vast array of fractal patterns in addition to tree-like structures. The versatility of fractal binary tree makes it a potential tool and important to the algorithmic study of complex natural design. Illustrations of the fractal binary tree include recursive grids, space-filling trees, and biological structures.

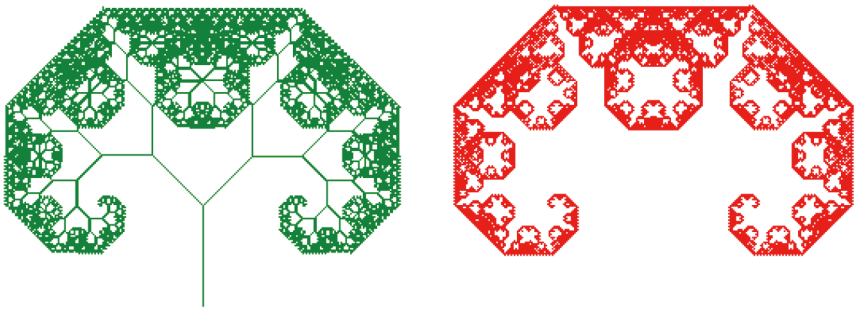

Figure 1. A symmetric binary tree with a branching angle of 45° and a scaling factor of $\frac{1}{\sqrt{2}}$ has branch extremities that generate a fractal that resembles the Lévy Dragon

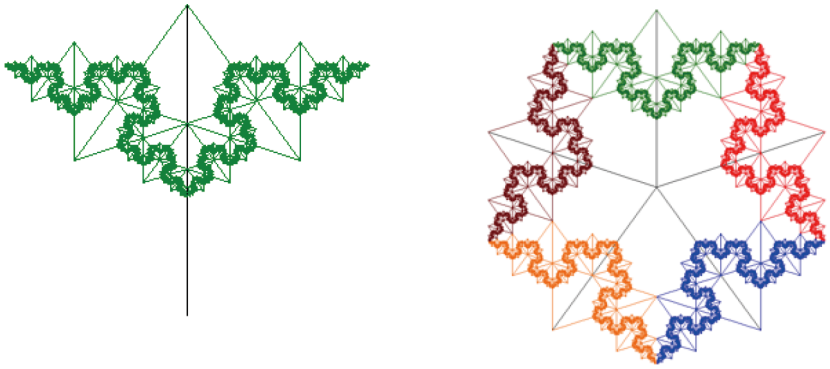

Figure 2. The golden 144° symmetric binary tree with a branching angle of 144° and a scaling factor of $\frac{2}{1+\sqrt{5}}$ with four additional copies rotated by 72° around the bottom of the trunk will form a "Golden Koch snowflake" with their branch tips

The intriguing continuation of fractal binary tree with increased complexity and a greater variety of potential forms and designs forms the fractal ternary tree. By adjusting the factors like scaling factor and branching angle, it replicates the wide range of natural designs making it a potential tool for investigation. Figure 3 shows the fractal fern is isomorphic to fractal ternary tree by adjusting the fractal characteristics like scaling factor and branching angle. The tree can easily change from one fractal form to another by gradually varying the angles or scaling factor. Self-similarity and Recursion capture the elegance of fractals perfectly. For instance, you can begin with a Koch Snowflake arrangement and transform it into a more fern-like structure by progressively increasing the branching angle. The Dragon Curve, Sierpinski Pyramid, Cantor Set, and Tetrahedral Fractal are some of the fractals that can also be generated by a fractal ternary tree.

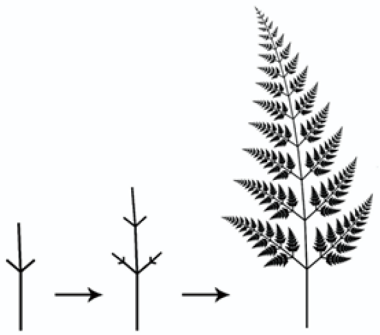

Figure 3. A fractal ternary tree resembles a fractal fern

Topological indices are generated from the graph-theoretical representation of molecules, networks, and other structures, with vertices representing atoms, nodes, or entities and edges representing bonds, connections, or relationships. Topological indices reduce complex structural information into numerical values by examining the patterns of adjacency and connectivity within these graphs. This information can be utilized in various fields such as machine learning, structure-activity relationship analysis, network analysis, molecular property prediction, complexity measurement, and simulation. We investigate the topological indices of fractal binary and ternary trees using vertex and edge partitioning of these respective graphs. The equivalence classes of vertex set and edge set helps in understanding of complex structures by simplifying into smaller sets. In chemical graph theory, each vertex replicates atoms and each edge replicates the bonds which is useful in analyzing the chemical properties. In network systems modeled by fractal trees, vertices represent

nodes, and edges represent links. Partitioning helps in understanding the critical nodes (e.g., root or central vertices) and vital connections (edges close to the root or between highly connected nodes).

Dendrimers are highly branched, tree-like polymers. Fractal trees serve as models for the graphical structure of dendrimer growth. The fractal nature of these trees provides a useful framework for understanding the hierarchical, self-similar structure of dendrimers, where each generation of branching closely resembles the overall structure [4–6]. Topological descriptors [7–15] derived from these trees are used in quantitative structure-activity relationship (QSAR) and quantitative structure-property relationship (QSPR) studies. Entropy quantifies the connectivity and branching complexity of dendrimers. The symmetry and recursive branching of fractal trees offer a robust theoretical foundation for advancing the development and application of dendrimers in these fields.

The topological analysis of fractal trees has not received sufficient attention. Since fractal binary and ternary trees are models for biological systems and highly branched chemical structures like dendrimers and polymers, it is crucial to investigate their topology as it advances the understanding of complex hierarchical structures. This contribution bridges theoretical graph analysis with real-world biological optimization. Our aim in this research is to work on the vertex and edge-level generalization of fractal binary and ternary trees, which simplifies the understanding of complex structures. For each of these trees, we analyze the degree-based topological descriptors and respected graph entropies, which are used to predict molecular properties in dendrimers and polymers, analyze hierarchical networks in communication and biological systems, measure complexity through entropy in diverse systems, and model natural systems such as vascular or ecological branching patterns. Finally, we compare the descriptors with their number of copies in the fractal dimension.

2. Preliminaries

2.1 *Topological descriptors*

Let $\mathscr{G}$ be the graph with vertex set $\mathscr{V}$ and edge set $\mathscr{E}$. The number of vertices incident with vertex v is called the degree of vertex v, it is denoted by $deg(v)$. The information regarding Randić index and its noteworthy characteristics are provided by Bollobás et al. [16] and Amić et al. [17]. The Randić index helps determine the bioactivity of chemical compounds, which aids in drug discovery. It also corresponds well with the heat of formation and hydrophobicity of molecules. Let α be any real number. R_α is referred to as the generalized Randić index, where $\alpha = \frac{1}{2}, -\frac{1}{2}$.

$$R_\alpha(\mathscr{G}) = \sum_{vw \in \mathscr{E}} (deg(v)deg(w))^\alpha \tag{2}$$

An early degree-based descriptor known as the first [18] and second Zagreb [19] indices was developed by Gutman and Trinajstić in 1972. Zagreb indices correlate with physicochemical properties like boiling points, melting points, and solubility of drugs using QSAR and QSPR studies. Also, it is used to predict the elasticity and conductivity of polymers and dendritic structures.

$$M_1(\mathscr{G}) = \sum_{vw \in \mathscr{E}} deg(v) + deg(w) \tag{3}$$

$$M_2(\mathscr{G}) = \sum_{vw \in \mathscr{E}} deg(v)deg(w) \tag{4}$$

The modified Zagreb index also called as Milan Randić index defined as

$$mM_2(\mathscr{G}) = \sum_{vw \in \mathscr{E}} \frac{1}{deg(v)deg(w)} \tag{5}$$

The Hyper Zagreb index is defined as

$$HM(\mathscr{G}) = \sum_{vw \in \mathscr{E}} (deg(v) + deg(w))^2 \tag{6}$$

Harmonic index [20] was given by Fajtlowicz. It contributes to chemical stability by assessing molecular interaction. It is defined as follows,

$$H(\mathscr{G}) = \sum_{vw \in \mathscr{E}} \frac{2}{deg(v) + deg(w)} \tag{7}$$

In 2015, Furtula and Gutman [21] defined the Forgotten Index. It provides insights into the branching complexity and reactivity of chemical compounds.

$$F(\mathscr{G}) = \sum_{vw \in \mathscr{E}} deg^2(v) + deg^2(w) \tag{8}$$

The inverse sum indeg index [22] is defined as

$$I(\mathscr{G}) = \sum_{vw \in \mathscr{E}} \frac{deg(v)deg(w)}{deg(v) + deg(w)} \tag{9}$$

The author of the article "Geometric approach to degree-based topological indices: Sombor indices" has proposed unique graph parameters based on vertex degree inspired by the Euclidean metric [23]. In a short period of time, researchers from all around the world have carried out multiple investigations using the Sombor index [24–29]. From the beginning, the Sombor index has had numerous modifications [30]. Additionally, there has been interest from researchers to examine modified versions of the Sombor index. Following earlier productive research on the Sombor index and its modifications, Gutman et al. [31] presented the Elliptic Sombor index, a novel vertex-degree-based topological index with geometric properties. Sombor indices are useful in evaluating structural compactness and strength in complex polymers. Also, it correlates well with thermodynamic properties of molecules.

$$SO(\mathscr{G}) = \sum_{vw \in \mathscr{E}} \sqrt{deg^2(v) + deg^2(w)} \tag{10}$$

$$SO_{red}(\mathscr{G}) = \sum_{vw \in \mathscr{E}} \sqrt{(deg(v) - 1)^2 + (deg(w) - 1)^2} \tag{11}$$

$$SO_{inc}(\mathscr{G}) = \sum_{vw \in \mathscr{E}} \sqrt{(deg(v)+1)^2 + (deg(w)+1)^2} \tag{12}$$

$$SO_{mod}(\mathscr{G}) = \sum_{vw \in \mathscr{E}} \frac{1}{\sqrt{deg^2(v) + deg^2(w)}} \tag{13}$$

$$KGSO(\mathscr{G}) = \sum_{vw \in \mathscr{E}} (\sqrt{deg^2(v) + (deg(v) + deg(w) - 2)^2} + \sqrt{deg^2(w) + (deg(v) + deg(w) - 2)^2}) \tag{14}$$

$$ESO(\mathscr{G}) = \sum_{vw \in \mathscr{E}} (deg(v) + deg(w))(\sqrt{deg^2(v) + deg^2(w)}) \tag{15}$$

2.2 *Graph entropy*

Graph entropy was introduced in an effort to characterize the complexity of graphs [32]. Its initial use was meant to highlight the complexity of interaction and knowledge transmission, but it is now widely used in many scientific domains [33]. Let us describe the entropy of a graph $\mathscr{G}$ when analyzed with the topological descriptor D as in [34],

$$ENT_D(\mathscr{G}) = -\sum_{z \in E(\mathscr{G})} p_z log(p_z) \tag{16}$$

$$ENT_D(\mathscr{G}) = log(D(\mathscr{G})) - \frac{1}{D(\mathscr{G})} \sum_{z \in E(\mathscr{G})} f(z) log(f_z) \tag{17}$$

3. Graphical representation of fractal binary tree graph

A fractal binary tree is a fractal structure with self-similar and symmetric properties. Here, each vertex gives birth to two child vertices. The left and right sub-trees are symmetric to each other. This symmetry, repeated at every level of the tree, results in a fractal pattern. The graphical representation of a fractal binary tree starts with a vertical trunk. From the vertex above, two child vertices are generated in a recursive manner. These trees are also observed in nature, modeling branching patterns like those of fir trees and river networks.

Let B_i be the graph of the fractal binary tree with i iterations. Then the cardinality of the vertex and edge sets of B_i are 2^{i+1} and $2^{i+1} - 1$. In a fractal binary tree, the vertices are of degree 1 or 3. The edges of a fractal binary tree are classified as $E(d_a, d_b)$, where ab identifies the edge, d_a represents the degree of vertex a, and d_b represents the degree of vertex b. Edges of the classifications $E(1, 3)$ and $E(3, 3)$ are included in the configuration; the cardinality of $E(1, 3)$ is $2^i + 1$, while the cardinality of $E(3, 3)$ is $2^i - 2$. Figure 4 displays the graphs of the fractal binary trees for $i = 1, 2, 3, 4$. The number of copies $N = 2$, since each vertex grows into 2 new vertices. If the new branch grows half the size of the parent branch, then the scaling factor $S = 2$. The fractal dimension of fractal binary tree FD with scaling factor 2 is 1. Reducing the value of the scaling factor results in the convergence of the fractal dimension value to 2. The value of fractal dimension depends on the value of the scaling factor and branching angle.

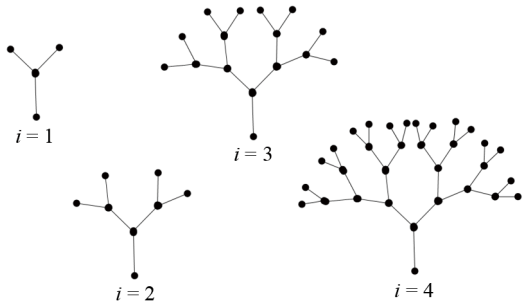

Figure 4. Fractal binary trees

4. Topological descriptors of fractal binary tree graph

Theorem 1 For the fractal binary tree B_i, $i > 1$ the degree-based topological descriptors are

1. $M_1(B_i) = 10 \times 2^i - 8$
2. $M_2(B_i) = 12 \times 2^i - 15$
3. $mM_2(B_i) = \frac{1}{9}(2^{i+2} + 1)$
4. $HM(B_i) = 52 \times 2^i - 56$
5. $H(B_i) = \frac{1}{6}(5 \times 2^i - 1)$
6. $F(B_i) = 28 \times 2^i - 26$
7. $I(B_i) = \frac{9}{4}(2^i - 1)$
8. For $\alpha = \frac{1}{2}, \frac{-1}{2}$; $R_\alpha(B_i) = 2^i(3^\alpha + 9^\alpha) + 3^\alpha - 2 \times 9^\alpha$
9. $SO(B_i) = 7.4049 \times 2^i - 5.3230$
10. $SO_{red}(B_i) = 4.8284 \times 2^i - 3.6569$
11. $SO_{inc}(B_i) = 10.1290 \times 2^i - 6.8416$
12. $SO_{mod}(B_i) = 0.5519 \times 2^i - 0.1552$
13. $KGSO(B_i) = 15.8416 \times 2^i - 14.1584$
14. $ESO(B_i) = 38.1050 \times 2^i - 38.2626$.

Theorem 2 For the fractal binary tree B_i, $i > 1$ the entropies are

1. $ENT_{M1}(B_i) = log(10 \times 2^i - 8) - \frac{1}{10 \times 2^i - 8}(4log(4)(2^i + 1) + 6log(6)(2^i - 2))$
2. $ENT_{M2}(B_i) = log(12 \times 2^i - 15) - \frac{1}{12 \times 2^i - 15}(3log(3)(2^i + 1) + 9log(9)(2^i - 2))$
3. $ENT_{mM2}(B_i) = log(\frac{1}{9}(2^{i+2} + 1) - \frac{9}{2^{i+2} + 1}(\frac{1}{3}log(\frac{1}{3})(2^i + 1) + \frac{1}{9}log(\frac{1}{9})(2^i - 2))$
4. $ENT_{HM}(B_i) = log(52 \times 2^i - 56) - \frac{1}{52 \times 2^i - 56}(32log(4)(2^i + 1) + 72log(6)(2^i - 2))$
5. $ENT_H(B_i) = log(\frac{1}{6}(5 \times 2^i - 1) - \frac{6}{5 \times 2^i - 1}(\frac{1}{2}log(2)(2^i + 1) + \frac{1}{3}log(3)(2^i - 2))$
6. $ENT_F(B_i) = log(28 \times 2^i - 26) - \frac{1}{28 \times 2^i - 26}(10log(10)(2^i + 1) + 18log(18)(2^i - 2))$
7. $ENT_I(B_i) = log(\frac{9}{4}(2^i - 1) - \frac{4}{9(2^i - 1)}(\frac{3}{4}log(\frac{3}{4})(2^i + 1) + \frac{3}{2}log(\frac{3}{2})(2^i - 2))$
8. For $\alpha = \frac{1}{2}, \frac{-1}{2}$; $R_\alpha(B_i) = log(3^\alpha(2^i + 1) + 9^\alpha(2^i - 2)) - \frac{1}{3^\alpha(2^i + 1) + 9^\alpha(2^i - 2)}(3^\alpha log(3^\alpha)(2^i + 1) + 9^\alpha log(9^\alpha)(2^i - 2))$
9. $ENT_{SO}(B_i) = log(7.4049 \times 2^i - 5.3230) - \frac{1}{7.4049 \times 2^i - 5.3230}(\sqrt{10}log(\sqrt{10})(2^i + 1) + \sqrt{18}log(\sqrt{18})(2^i - 2))$

10. $ENT_{SO_{red}}(B_i) = log(4.8284 \times 2^i - 3.6569) - \frac{1}{4.8284 \times 2^i - 3.6569}(2log(2)(2^i+1) + \sqrt{8}log(\sqrt{8})(2^i-2))$

11. $ENT_{SO_{inc}}(B_i) = log(10.1290 \times 2^i - 6.8416) - \frac{1}{10.1290 \times 2^i - 6.8416}(\sqrt{20}log(\sqrt{20})(2^i+1) + \sqrt{32}log(\sqrt{32})(2^i - 2))$

12. $ENT_{SO_{mod}}(B_i) = log(0.5519 \times 2^i - 0.1552) - \frac{1}{0.5519 \times 2^i - 0.1552}(\frac{1}{\sqrt{10}}log(\frac{1}{\sqrt{10}})(2^i+1) + \frac{1}{\sqrt{18}}log(\frac{1}{\sqrt{18}})(2^i - 2))$

13. $ENT_{KGSO}(B_i) = log(15.8416 \times 2^i - 14.1584) - \frac{1}{15.8416 \times 2^i - 14.1584}((\sqrt{5}+\sqrt{13})log(\sqrt{5}+\sqrt{13})(2^i + 1) + 10log(10)(2^i - 2))$

14. $ENT_{ESO}(B_i) = log(38.1050 \times 2^i - 38.2626) - \frac{1}{38.1050 \times 2^i - 38.2626}(4\sqrt{10}log(4\sqrt{10})(2^i+1) + 18\sqrt{2}log(18\sqrt{2})(2^i - 2))$.

5. Comparison of topological descriptors of B_i

Using the descriptors, Figure 5 and Figure 6 presents the comparison graphs for the fractal binary tree B_i for a given i sequence. The iteration count i and the predicted topological descriptors for the B_i sequences are shown on the horizontal and vertical axes, respectively. In the graphs, each topological descriptor is indicated separately. The graphs demonstrate how all the descriptor values rise in parallel with the number of iterations i. When comparing the amount of replicas in the fractal dimension of the fractal binary tree, all topological descriptors yield replicas of two for every i.

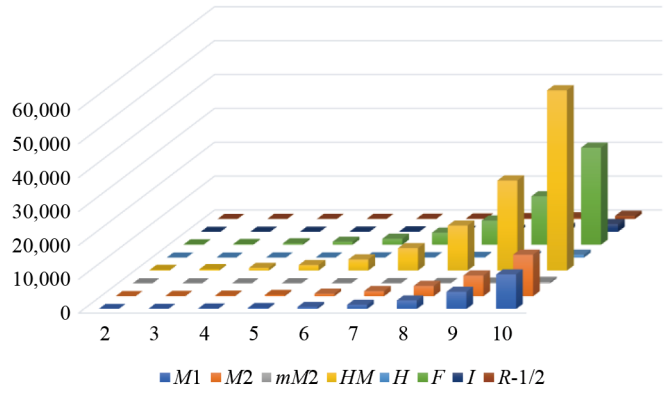

Figure 5. Graphical comparison of topological descriptors of B_i

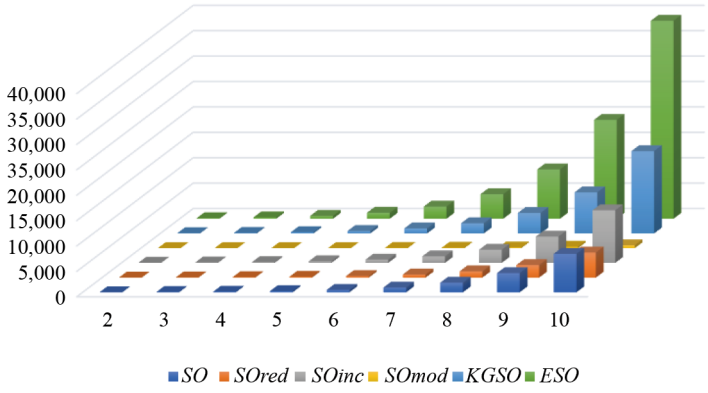

Figure 6. Graphical comparison of sombor indices of B_i

In Figure 7 and 8, the graphical comparison of topological entropies and sombor entropies for the fractal binary tree are given. These findings show that the entropy value increases with respect to the iteration value i of B_i. Additionaly compared to other topological entropies, ENT_{M1} develop faster when the structure grows and ENT_{ESO} develop slower compared to other sombor entropies of B_i.

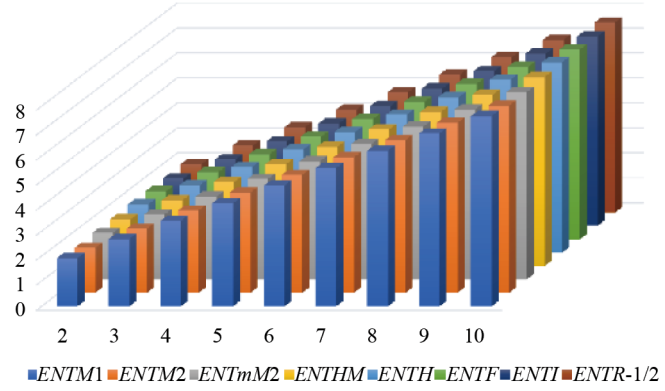

Figure 7. Graphical comparison of topological entropies of B_i

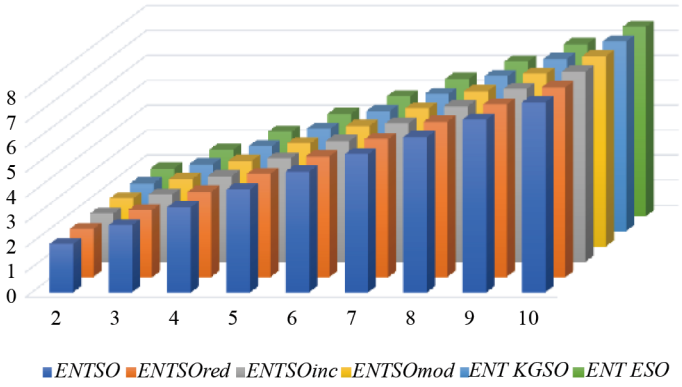

Figure 8. Graphical comparison of sombor entropies of B_i

6. Graphical representation of fractal ternary tree graph

A fractal ternary tree begins from a single trunk with two vertices. From the top vertex, it splits into three new branches symmetrically. For instance, if viewed from the top, the three branches might be evenly spaced around the trunk, forming angles like 120 degrees between each pair. Each of the three branches at the first level itself becomes a trunk for three new branches in the next iteration. This branching continues recursively, meaning that each new branch generates three smaller branches, maintaining the symmetric arrangement. Typically, the length of each new set of branches is a fraction of the branches in previous level. Due to the scaling property, the tree looks same as it develops. For example, if the initial branch length is l, the branches at the next level might be $l/2$, and those at the following level $l/4$, and so on. The fractal ternary tree exhibits radial symmetry and self-similar fractal properties. Since the new branches grow at equal angles in all levels of recursion and each branch or segment of the tree resembles the entire tree.

Let T_n be the graph of fractal ternary tree with n iterations. Because of the complexity of structure, sequences are used for generalization of vertex and edge sets. Consider a sequence v_n with $v_2 = 14$, then the total number of the vertex set is given by $(3 \times v_{n-1}) - 1$. Similarly, consider a sequence e_n with $e_2 = 13$, then the total number of edge set is $(3 \times a_{n-1}) + 1$.

In a fractal ternary tree, the vertices are of degree 1 or 4. The edges of a fractal ternary tree are classified as $E(1,\ 4)$ and $E(4,\ 4)$. Let a_n and b_n be two other sequences with $a_2 = 10$ and $b_2 = 3$, then $3 \times (a_{n-1} - 1) + 1$ is the cardinality of the edge set $E(1,\ 4)$ and $(3 \times b_{n-1}) + 3$ is the cardinality of $E(4,\ 4)$. Figure 9 depicts the graphs of fractal ternary trees for $n = 1, 2, 3$. Every branch in a fractal ternary tree divides into three new branches. Thus, $N = 3$. The value assigned to the branches determines the scaling factor S. $S = 2$ if every new branch is scaled by half of its branch size of the parent. For fractal ternary tree, the fractal dimension FD is 1.585 with scaling factor 2. The exact fractal dimension values are determined by the branching angles, particular scaling algorithms, and degree of complexity or randomness in the structure of fractal ternary tree.

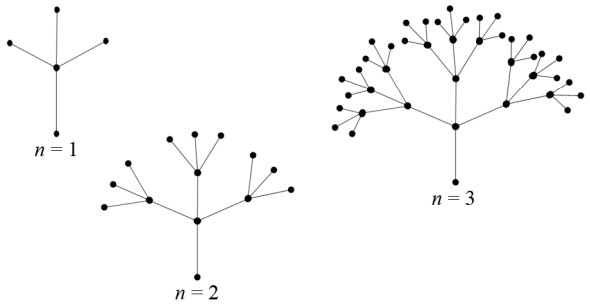

Figure 9. Fractal ternary trees

7. Topological descriptors of fractal ternary tree graph

Theorem 3 For the fractal ternary tree T_n, where $n > 1$, $a_2 = 10$, $b_2 = 3$ the degree-based topological descriptors follows,

1. $M_1(T_n) = 15 \times (a_{n-1} - 1) + 24 \times b_{n-1} + 29$
2. $M_2(T_n) = 12 \times (a_{n-1} - 1) + 48 \times b_{n-1} + 52$
3. $mM_2(T_n) = 0.75 \times (a_{n-1} - 1) + 0.1875 \times b_{n-1} + 0.4375$
4. $HM(T_n) = 75 \times (a_{n-1} - 1) + 192 \times b_{n-1} + 217$
5. $H(T_n) = 1.2 \times (a_{n-1} - 1) + 0.75 \times b_{n-1} + 1.15$
6. $F(T_n) = 51 \times (a_{n-1} - 1) + 96 \times b_{n-1} + 113$
7. $I(T_n) = 2.4 \times (a_{n-1} - 1) + 6 \times b_{n-1} + 6.8$
8. For $\alpha = \frac{1}{2},\ \frac{-1}{2}$; $R_\alpha(T_n) = 3 \times 4^\alpha \times (a_{n-1} - 1) + 3 \times 4^{2\alpha} \times b_{n-1} + 4^\alpha + 3 \times 4^{2\alpha}$
9. $SO(T_n) = 12.3693 \times (a_{n-1} - 1) + 16.9706 \times b_{n-1} + 21.0937$
10. $SO_{red}(T_n) = 9 \times (a_{n-1} - 1) + 12.7279 \times b_{n-1} + 15.7279$
11. $SO_{inc}(T_n) = 16.1555 \times (a_{n-1} - 1) + 21.2132 \times b_{n-1} + 26.5984$
12. $SO_{mod}(T_n) = 0.7276 \times (a_{n-1} - 1) + 0.5303 \times b_{n-1} + 0.7729$
13. $KGSO(T_n) = 24.4868 \times (a_{n-1} - 1) + 43.2666 \times b_{n-1} + 51.4289$
14. $ESO(T_n) = 61.8466 \times (a_{n-1} - 1) + 135.7645 \times b_{n-1} + 156.3800.$

Theorem 4 For the fractal ternary tree T_n, where $n > 1$, $a_2 = 10$, $b_2 = 3$ the entropies are

1. $ENT_{M_1}(T_n) = log(M_1(T_n)) - \frac{1}{M_1(T_n)}(5log(5)(3(a_{n-1} - 1) + 1) + 8log(8)(3b_{n-1} + 3))$
2. $ENT_{M_2}(T_n) = log(M_2(T_n)) - \frac{1}{M_2(T_n)}(4log(4)(3(a_{n-1} - 1) + 1) + 16log(16)(3b_{n-1} + 3))$
3. $ENT_{mM_2}(T_n) = log(mM_2(T_n)) - \frac{1}{mM_2(T_n)}(\frac{1}{4}log(\frac{1}{4})(3(a_{n-1} - 1) + 1) + \frac{1}{16}log(\frac{1}{16})(3b_{n-1} + 3))$
4. $ENT_{HM}(T_n) = log(HM(T_n)) - \frac{1}{HM(T_n)}(25log(25)(3(a_{n-1} - 1) + 1) + 64log(64)(3b_{n-1} + 3))$

5. $ENT_H(T_n) = log(H(T_n)) - \frac{1}{H(T_n)}(\frac{2}{5}log(\frac{2}{5})(3(a_{n-1}-1)+1) + \frac{1}{4}log(\frac{1}{4})(3b_{n-1}+3))$

6. $ENT_F(T_n) = log(F(T_n)) - \frac{1}{F(T_n)}(17log(17)(3(a_{n-1}-1)+1) + 32log(32)(3b_{n-1}+3))$

7. $ENT_I(T_n) = log(I(T_n)) - \frac{1}{I(T_n)}(\frac{4}{5}log(\frac{4}{5})(3(a_{n-1}-1)+1) + 2log(2)(3b_{n-1}+3))$

8. For $\alpha = \frac{1}{2}, \frac{-1}{2}$; $ENT_{R_\alpha}(T_n) = log(R_\alpha(T_n)) - \frac{1}{R_\alpha(T_n)}(4^\alpha log(4^\alpha)(3(a_{n-1}-1)+1) + 16^\alpha log(16^\alpha)(3b_{n-1}+3))$

9. $ENT_{SO}(T_n) = log(SO(T_n)) - \frac{1}{SO(T_n)}(\sqrt{17}log(\sqrt{17})(3(a_{n-1}-1)+1) + 4\sqrt{2}log(4\sqrt{2})(3b_{n-1}+3))$

10. $ENT_{SO_{red}}(T_n) = log(SO_{red}(T_n)) - \frac{1}{SO_{red}(T_n)}(3log(3)(3(a_{n-1}-1)+1) + 3\sqrt{2}log(3\sqrt{2})(3b_{n-1}+3))$

11. $ENT_{SO_{inc}}(T_n) = log(SO_{inc}(T_n)) - \frac{1}{SO_{inc}(T_n)}(\sqrt{29}log(\sqrt{29})(3(a_{n-1}-1)+1) + 5\sqrt{2}log(5\sqrt{2})(3b_{n-1}+3))$

12. $ENT_{SO_{mod}}(T_n) = log(SO_{mod}(T_n)) - \frac{1}{SO_{mod}(T_n)}(\frac{1}{\sqrt{17}}log(\frac{1}{\sqrt{17}})(3(a_{n-1}-1)+1) + \frac{1}{4\sqrt{2}}log(\frac{1}{4\sqrt{2}})(3b_{n-1}+3))$

13. $ENT_{KGSO}(T_n) = log(KGSO(T_n)) - \frac{1}{KGSO(T_n)}((5+\sqrt{10})log(5+\sqrt{10})(3(a_{n-1}-1)+1) + 4\sqrt{13}log(4\sqrt{13})(3b_{n-1}+3))$

14. $ENT_{ESO}(T_n) = log(ESO(T_n)) - \frac{1}{ESO(T_n)}(5\sqrt{17}log(5\sqrt{17})(3(a_{n-1}-1)+1) + 32\sqrt{2}log(32\sqrt{2})(3b_{n-1}+3))$.

8. Comparison of topological descriptors of T_n

The two comparison graphs for the fractal ternary tree T_n for a specific n succession are displayed in Figure 10 and Figure 11 using the topological descriptors. The horizontal axis displays the iteration number n, while the vertical axis displays the projected topological descriptors for T_n. Each topological descriptor is displayed independently in the graphs. The graphs show how the descriptor values increase simultaneously with the iteration number, n. There are three replicas for every n for all topological descriptors when analyzing the number of replicas in the fractal dimension.

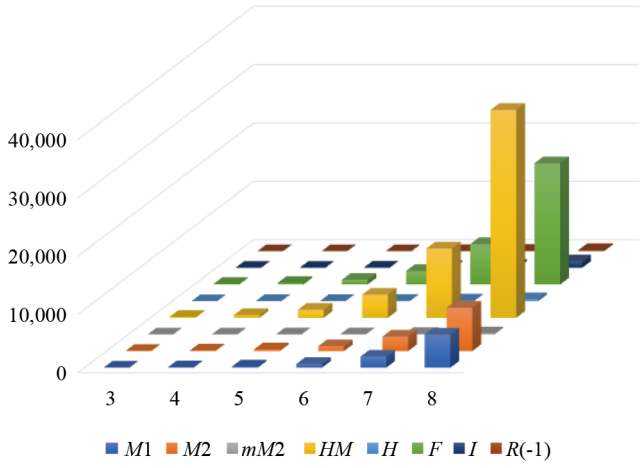

Figure 10. Graphical representation of topological descriptors of T_n

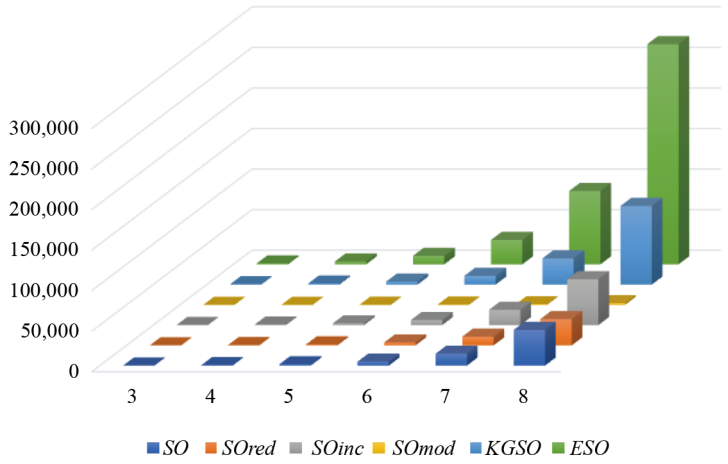

Figure 11. Graphical representation of sombor indices of T_n

The topological entropies and sombor entropies for the fractal ternary tree are graphically compared in Figures 12 and 13. These results show that the entropy value increases in relation to the iteration value n of T_n. Furthermore, when the structure evolves, ENT_{M1} evolves rapidly compared to other topological entropies, while ENT_{ESO} develops gradually compared to other entropies of T_n.

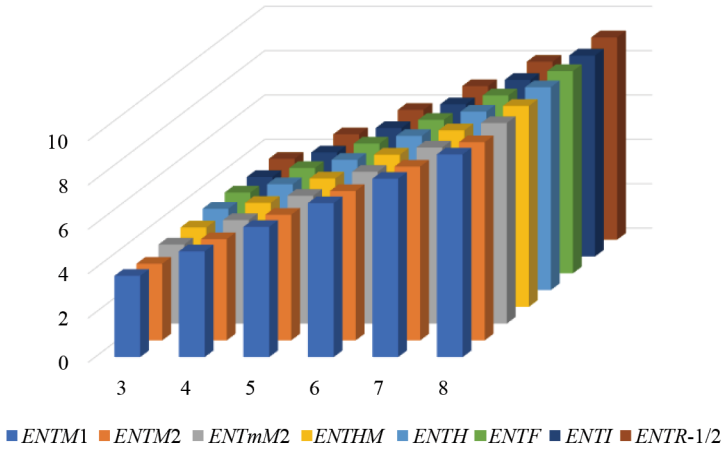

Figure 12. Graphical representation of topological entropies of T_n

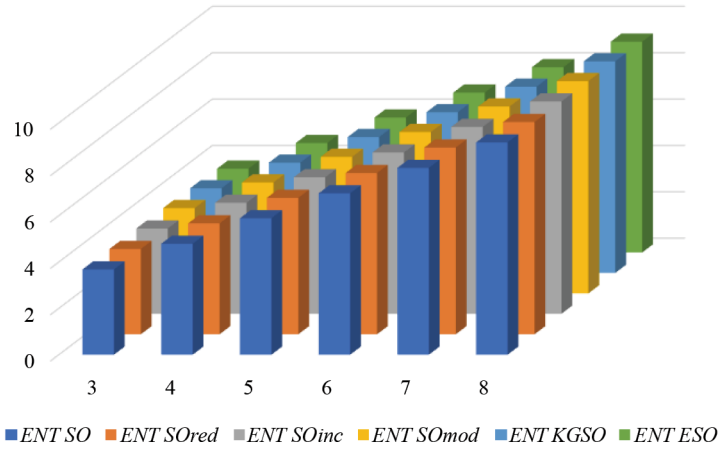

Figure 13. Graphical representation of sombor entropies of T_n

9. Application

The computation of topological indices and graph entropies for the fractal binary and ternary trees has applications in numerous fields. Especially in material science, fractal trees are isomorphic to dendritic crystals and nanomaterials. Topological indices of fractal trees are used in the introduction of nanoparticles since they determine the rate of diffusion and thermal resistance. Also, they are associated with the structural integrity of fractal architectures. Graph entropy, which measures the degree of disorder or uniformity in material composition, aids in the formation of amorphous and composite materials. In biology, fractal trees are used to model neuronal sprouting and vascular networks. It can also represent genetic branching in species phylogenies. The indicators help analyze the efficiency of signal or nutrient transfer and evaluate the robustness and resilience of networks. It also makes it easier to understand the biological interconnections and the structural complexity of genetic trees. In the field of drug delivery, fractal trees behave as models for dendrimers, which helps to correlate their physicochemical properties using topological indices of fractal trees. Entropy measures the structural complexity and quantifies the drug delivery patterns. Also, topological indices of fractal trees are utilized in the field of network architecture, like peer-to-peer networks and distributed systems. Fractal trees are recursive data structures, which makes them useful in decision trees and search algorithms. Figure 14 summarizes the critical role of topological indices and entropy in predicting, analyzing, and optimizing properties across diverse disciplines.

Field	TopologicalIndices	Graph entropy
Material Science	Predict diffusion rates, mechanical properties	Measure complexity in nanoporous materials
Biology	Analyzenutrient transport, network resilience	Quantify diversity in biological systems
Dendrimer Formation	Model size, branching density in dendrimers	Optimize drug delivery and structural design
Computer Science	Optimize recursive algorithms, network topology	Evaluate algorithmic complexity, traffic flow

Figure 14. Application of topological indices and entropy measures of fractal trees in various disciplines

10. Conclusion

The present research explores a variety of topological descriptors and entropy measures for the fractal graphs, including the Zagreb indices, Forgotten index, Inverse sum indeg index, general Randić index, Sombor indices, and their respective entropies. The article also includes graphs comparing all the topological descriptors and entropy measures for each fractal graph. It is important to note that every topological descriptor offers three copies for fractal ternary trees and two copies for fractal binary trees. The empirical data fitting method will demonstrate the effectiveness of the proposed work by comparing computed indices and entropy values with experimental data from materials, biological systems, or networks to validate models. In our future work, we intend to look into the topological characteristics of different fractal networks having complex structures as the iteration increases. This work contributes to chemical graph theory and related disciplines by offering analytical expressions and highlighting potential applications in molecular modeling, network theory, and information science.

Conflict of interest

The authors declare that they have no conflict of interest.

References

[1] Mandelbrot B. *The Fractal Geometry of Nature*. New York; 1982.

[2] Mendler N, Matsko VJ. Symmetric binary trees with branching ratios larger than 1. In: *Proceedings of Bridges 2017: Mathematics, Art, Music, Architecture, Education, Culture.* The Bridges Archive; 2017. p.507-510.

[3] Pons BE. Unfolding symmetric fractal trees. In: *Proceedings of Bridges 2013: Mathematics, Music, Art, Architecture, Culture.* The Bridges Archive; 2013. p.295-302.

[4] Pippa N, Dokoumetzidis A, Demetzos C, Macheras P. On the ubiquitous presence of fractals and fractal concepts in pharmaceutical sciences: A review. *Ternational Journal of Pharmaceutics*. 2013; 456(2): 340-352.

[5] Rian IM, Sassone M. Tree-inspired dendriforms and fractal-like branching structures in architecture: A brief historical overview. *Frontiers of Architectural Research*. 2014; 3(3): 298-323.

[6] Klajnert B, Bryszewska M. Dendrimers: Properties and applications. *Acta Biochimica Polonica*. 2001; 48(1): 199-208.

[7] Thanga Rajeswari K, Manimaran A. The sombor indices of banana tree graph and fractal tree type dendrimer. *Contemporary Mathematics*. 2024; 5(3): 4079-4094.

[8] Ishfaq F, Nadeem MF. Topological properties of fractals via M-polynomial. *Arabian Journal of Mathematics.* 2024; 13: 303-317.

[9] Jyothish K, Santiago R, Govardhan S, Hayat S. Structure-property modeling of physicochemical properties of fractal trigonal triphenylenoids by means of novel degree-based topological indices. *The European Physical Journal E.* 2024; 47(6): 42.

[10] Divya A, Manimaran A. Topological indices for the iterations of Sierpiński rhombus and Koch snowflake. *The European Physical Journal Special Topics*. 2021; 230: 3971-3980.

[11] Sattar A, Javaid M, Abebe Ashebo M. On the comparative analysis among topological indices for rhombus silicate and oxide structures. *Journal of Mathematics*. 2024; 2024(1): 2773913.

[12] Nadeem M, Kamran M, Alhazmi M, Alsaeedi M, Hilali SO. Topology of quasi divisor graphs associated with non-associative algebra. *Ain Shams Engineering Journal*. 2024; 15(12): 103123.

[13] Nadeem M, Alam MA, Ali N, Elashiry MI. An algebraic approach of topological indices connected with finite quasigroups. *Journal of Function Spaces*. 2024; 2024(1): 1948465.

[14] Nadeem M, Siddique I, Alam MA, Ali W. A new graphical representation of the old algebraic structure. *Journal of Mathematics*. 2023; 2023(1): 4333301.

[15] Nadeem M, Ahmad S, Siddiqui MK, Naeem M. Topological descriptor of 2-dimensional silicon carbons and their applications. *Open Chemistry*. 2019; 17(1): 1473-1482.

[16] Bollobás B, Erdös P. Graphs of extremal weights. *Ars Combinatoria*. 1998; 50: 225.
[17] Amić D, Beslo D, Lucić B, Nikolić S, Trinajstić N. The vertex-connectivity index revisited. *Journal of Chemical Information and Computer Sciences*. 1998; 38(5): 819-822.
[18] Gutman I, Das K. The first Zagreb index 30 years after. *MATCH Communications in Mathematical and in Computer Chemistry*. 2004; 50(1): 83-92.
[19] Gutman I, Trinajstić N. Graph theory and molecular orbitals. Total φ-electron energy of alternant hydrocarbons. *Chemical Physics Letters*. 1972; 17(4): 535-538.
[20] Fajtlowicz S. On conjectures of Graffiti-II. *Congressus Numerantium*. 1987; 60: 187-197.
[21] Furtula B, Gutman I. A forgotten topological index. *Journal of Mathematical Chemistry*. 2015; 53(4): 1184-1190.
[22] Sedlar J, Stevanovic D, Vasilyev A. On the inverse sum indeg index. *Discrete Applied Mathematics.* 2015; 184: 202-212.
[23] Gutman I. Geometric approach to degree-based topological indices: Sombor indices. *Communications in Mathematical and in Computer Chemistr*. 2021; 86(1): 11-16.
[24] Redˇzepović I. Chemical applicability of Sombor indices: Survey. *Journal of Serbian Chemical Society*. 2021; 86(5): 445-457.
[25] Das KC, Çevik AS, Cangul IN, Shang Y. On sombor index. *Symmetry*. 2021; 13(1): 140.
[26] Milovanovic I, Milovanovic E, Matejic M. On some mathematical properties of Sombor indices. *Bulletin of the International Mathematical Virtual Institute*. 2021; 11(2): 341-353.
[27] Redžepović I. Chemical applicability of Sombor indices. *Journal of the Serbian Chemical Society*. 2021; 86(5): 445-457.
[28] Shanmukha MC, Usha A, Kulli VR, Shilpa KC. Chemical applicability and curvilinear regression models of vertex-degree-based topological index: Elliptic Sombor index. *International Journal of Quantum Chemistry*. 2024; 124(9): e27376.
[29] Hayat S, Arshad M, Khan A. Graphs with given connectivity and their minimum Sombor index having applications to QSPR studies of monocarboxylic acids. *Heliyon*. 2024; 10(1): e23392.
[30] Kulli VR. Different versions of Sombor index of some chemical structures. *International Journal of Engineering Sciences and Research Technology*. 2021; 10(7): 23-32.
[31] Gutman I, Furtula B, Oz MS. Geometric approach to vertex degree based topological indices-Elliptic Sombor index, theory and application. *International Journal of Quantum Chemistry*. 2024; 124(2): e27346.
[32] Mowshowitz A, Dehmer M. Entropy and the complexity of graphs revisited. *Entropy*. 2012; 14(3): 559-570.
[33] Sabirov DS, Shepelevich IS. Information entropy in chemistry: An overview. *Entropy*. 2021; 23(10): 1240.
[34] Kazemi R. Entropy of weighted graphs with the degree-based topological indices as weights. *MATCH Communications in Mathematical and in Computer Chemistry*. 2016; 76(1): 69-80.